Journal of Inorganic and Organometallic Polymers and Materials (2024) 34:3028–3036
https://doi.org/10.1007/s10904-024-03125-0

RESEARCH

Polyplatinaynes Functionalized with Pyrazoline Derivatives

Qiwei Wang[1,2] · Lu Jiang[1] · Junlong Li[1] · Zelin Sun[3] · Wai-Yeung Wong[2,3,4]

Received: 27 April 2024 / Accepted: 3 May 2024 / Published online: 17 June 2024
© The Author(s) 2024

Abstract
Pyrazoline and pyrazole compounds are important building blocks in the development of photofunctional compounds. Two new solution-processable platinum-containing polyynes functionalized with these chromophores in the main chain (**P1** and **P2**) were synthesized and characterized by spectroscopic, thermal and optical methods. By changing the spacer from 2-pyrazoline to the electron-rich pyrazole in the main chain, the photophysical properties including energy levels, absorption wavelength and bandgap of the polymers were finely tuned. The photovoltaic properties of **P1** with better absorption features were also studied.

Graphical abstract

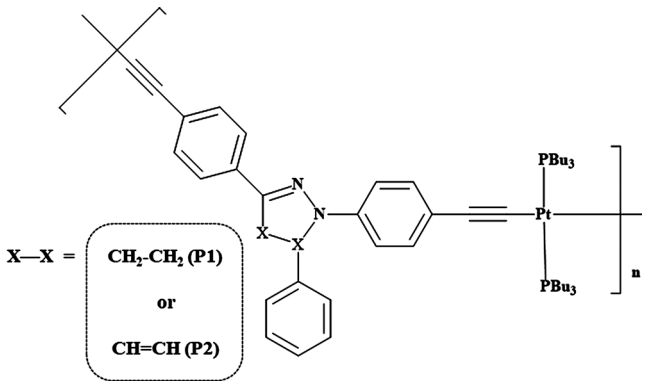

Keywords Metallopolymer · Platinum · Pyrazoline · Pyrazole · Synthesis

✉ Wai-Yeung Wong
wai-yeung.wong@polyu.edu.hk

Qiwei Wang
wqw@cioc.ac.cn

Zelin Sun
zelin689.sun@polyu.edu.hk

1 Antibiotics Research and Reevaluation Key Laboratory of Sichuan Province, Sichuan Industrial Institute of Antibiotics, Chengdu University, Chengdu 610052, P. R. China

2 Department of Chemistry, Hong Kong Baptist University, Waterloo Road, Kowloon Tong, Hong Kong, P. R. China

3 Department of Applied Biology and Chemical Technology, The Hong Kong Polytechnic University (PolyU), Hong Kong, Hung Hom, P. R. China

4 PolyU Shenzhen Research Institute, Shenzhen 518057, P. R. China

1 Introduction

The development of transition metal polyynes of the form *trans*-$[-M(L)_2-C\equiv C-Ar-C\equiv C-]_n$ (L = auxiliary ligands, Ar = spacer unit) has shown much progress in the past few decades [1–5]. These main-chain organometallic polymers are useful functional materials for luminescence, photovoltaics, biology, nonlinear optics (NLO) and chemosensing [1–6]. To date, a large family of soluble platinum(II) polyynes incorporating various conjugated carbocyclic and heteroaromatic ring systems is known [7–12].

2-Pyrazoline derivatives are good candidates for constructing versatile optical materials [13–16]. These compounds show fluorescence and electrooptical properties and by means of easy synthetic procedures, allow the introduction of appropriate substituents for tailoring the second-order

NLO properties. In particular, 1,3,5-triaryl-2-pyrazoline derivatives have been studied due to their high photoluminescence and good electrochemical activity and are widely applied as fluorescent probes, NLO materials and OLED materials [17]. Pyrazoline has an interesting ring containing both an electron-accepting imine –C = N– group and an electron-donating –N(Ar)– group. The N atom of pyrazoline attains conjugation by electron donation which leads to higher hole-transport efficiency and some photoelectron characteristics [13]. Therefore, the pyrazoline derivatives are expected to be used as a new type of optoelectronic materials in a broader field of applications. On the other hand, the electron-rich pyrazoles are an important class of nitrogen-containing five-membered heterocycles and show a range of applications in medicine, dye-sensitized solar cells and second-order NLO [18–25]. To our knowledge, there are no reports on exploiting pyrazoline and its pyrazole derivatives in the preparation of organometallic polyynes. In this work, two new polyplatinayne polymers (**P1** and **P2**) were designed and synthesized, which contain structurally similar pyrazoline and pyrazole rings in the polymer main chain.

2 Experimental Section

2.1 Materials and Instruments

All the chemicals were purchased from Acros or Aldrich and used as received unless otherwise specified. *trans*-$[Pt(PBu_3)_2Cl_2]$ [26] was prepared using the methods reported in the literature. THF was dried by distillation from sodium with benzophenone as an indicator under a nitrogen atmosphere. Separation and purification of products were achieved by column chromatography on silica gel. TLC was carried out in air using laboratory grade solvents as eluents.

The positive-ion fast atom bombardment (FAB) mass spectra were recorded in *m*-nitrobenzyl alcohol matrices on a Finngin-MAT SSQ710 mass spectrometer. Infrared spectra were recorded on the Nicolet Magna 550 Series II FTIR spectrometer using KBr pellets for solid state spectroscopy. NMR spectra were measured in deuterated solvents as the lock and reference on Varian INOVA 400 instrument or Bruker AV 400 MHz FT-NMR spectrometer, with ^{1}H and ^{13}C NMR chemical shifts quoted relative to Me_4Si standard and ^{31}P chemical shifts relative to an 85% H_3PO_4 external reference. Electronic absorption spectra were obtained with a Hewlett Packard 8453 spectrometer. Solution state photoluminescence measurements were obtained by the LS50B fluorescent spectrometer. For lifetime measurements, the third harmonics, 355 nm line of a Q-switched Nd: YAG laser was used as the excitation light source. The emission was recorded by using a PMT and an HP54522A 500 MHz oscilloscope. The PL spectra were measured in CH_2Cl_2 with a PTI Fluorescence Master Series QM1 spectrophotometer. The molecular weights of the polymers were determined by gel permeation chromatography (GPC) (HP 1050 series HPLC with visible wavelength and fluorescent detectors) using polystyrene standards. Thermal analysis was performed with a Perkin-Elmer TGA6 thermal analyzer.

The cyclic voltammograms were acquired with a CHI model 600D electrochemical station in deoxygenated acetonitrile containing 0.1 M $[Bu_4N]PF_6$ as the supporting electrolyte. A conventional three-electrode configuration consisting of a platinum working electrode, a Pt-wire counter electrode and an Ag/AgCl reference electrode was used. The polymer films were cast on the ITO covered glass. All potentials reported were quoted with reference to the ferrocene-ferrocenium (Fc/Fc^+) couple at a scan rate of 100 mV s^{-1}.

2.2 Fabrication and Characterization of Polymer Solar Cells

PCBM was purchased from American Dyes while PEDOT/PSS (Baytron P VPAI 4083) was purchased from H. C. Starck. Device configuration of ITO/poly(3,4-ethylenedioxythiophene):poly(styrene sulfonate) (PEDOT:PSS)/polymer:PCBM/Al was applied in this study. Indium tin oxide (ITO) coated glass substrates (10 Ω per square) were cleaned by sonication in toluene, acetone, ethanol, and deionized water, dried in an oven, and then cleaned with UV ozone for 300 s. As-received PEDOT: PSS solution was passed through the 0.45 μm filter and spin-coated on patterned ITO substrates at 5000 rpm for 3 min, followed by baking in N_2 at 150 °C for 15 min. **P1**:PCBM (1:4 by weight) active layer was prepared by spin-coating the toluene solution (4 mg mL^{-1} of **P1** and 16 mg mL^{-1} of PCBM) at 800 rpm for 2 min. The substrates were dried at room temperature under vacuum for 1 h and then stored under high vacuum (10^{-5} to 10^{-6} Torr) overnight. An Al electrode (100 nm) was evaporated through a shadow mask to define the active area of the devices (2 mm^2 circle). All the fabrication procedures (except drying, PEDOT:PSS annealing and Al deposition) and cell characterization were performed in air. Power conversion efficiency (PCE) was determined from *J*–*V* curve measurement (using a Keithley 2400 sourcemeter) under white light illumination (at 100 mW cm^{-1}). For white light efficiency measurements, an Oriel 66,002 solar light simulator with an AM1.5 filter was used. The light intensity was measured by a Molectron Power Max 500D laser power meter. For the measurement of the external quantum efficiency (EQE), different wavelengths were selected with an Oriel Cornerstone 74,000 monochromator, while the photocurrent was measured with a Keithley

2400 sourcemeter. The light intensity was measured with a Newport 1830-C optical power meter equipped with an 818-UV detector probe.

2.3 General Procedures for the Synthesis of Polyplatinayne Polymers P1 and P2

2.3.1 Synthesis of 1-(4-bromophenyl)-3-phenylprop-2-en-1-one

In 100 mL round-bottom flask, benzaldehyde (1.2 mL, 11.80 mol) was dissolved in absolute alcohol (32 mL) at room temperature. After 2.5 M NaOH (32 mL) was added, 1-(4-bromophenyl)ethanone (2.40 g, 12.06 mmol) was added and the resulting mixture was stirred for 3 h at room temperature. The precipitate was collected, washed with ice-cooled water and recrystallized from ethanol and dried to obtain 1-(4-bromophenyl)-3-phenylprop-2-en-1-one (3.40 g, 11.84 mmol, 88%) as a pale yellow solid. ^{1}H NMR (400 MHz, $CDCl_3$): δ = 7.91–7.89 (m, 2 H, Ar), 7.83 (m, 1H, Ar), 7.67–7.64 (m, 4 H, Ar), 7.51–7.46 (m, 1H, CH = CH), 7.44 (m, 3 H, Ar + CH = CH) ppm. ^{13}C NMR (100 MHz, $CDCl_3$): δ = 189.43 (C = O), 145.47, 136.89, 134.65, 131.96, 130.81, 129.04, 128.55, 127.94, 121.42 (Ar + C = C) ppm. FAB-MS: *m/z* = 289.1 $[M]^+$.

2.3.2 Synthesis of 1,3-bis(4-bromophenyl)-5-phenyl-4,5-dihydro-1*H*-pyrazole L1-Br

A mixture of 1-(4-bromophenyl)-3-phenylprop-2-en-1-one (1.63 g, 5.66 mmol) and 1-bromophenylhydrazine hydrochloride (1.27 g, 5.66 mmol) in 20 mL ethanol was heated to reflux for 24 h under a nitrogen atmosphere. After the mixture was cooled down to room temperature, the precipitate was collected and washed with ethanol and dried to obtain **L1-Br** (2.30 g, 5.05 mmol, 89%) as a yellow solid. ^{1}H NMR (400 MHz, $CDCl_3$): δ = 7.58–7.56 (m, 2 H, Ar), 7.52–7.49 (m, 2 H, Ar), 7.34–7.32 (m, 2 H, Ar), 7.29–7.27 (m, 2 H, Ar), 7.26–7.24 (m, shielded by $CHCl_3$ proton, 2 H, Ar), 6.93–6.90 (m, 2 H, Ar), 5.28–5.24 (m, 1H, CH), 3.86–3.78 (m, 1H, CH_2), 3.15–3.09 (m, 1H, CH_2) ppm. ^{13}C NMR (100 MHz, $CDCl_3$): δ = 146.25, 143.37. 141.68, 131.75, 131.71, 131.38, 129.31, 127.89, 127.20, 125.75, 122.82, 114.95, 111.40 (Ar + C = N), 64.40 (CH-N), 43.43 (CH_2) ppm. FAB-MS: *m/z* = 455.9 $[M]^+$.

2.3.3 Synthesis of L1-TMS

To an ice-cooled mixture of **L1-Br** (500 mg, 1.09 mmol) in freshly distilled triethylamine (20 mL) and CH_2Cl_2 (20 mL) solution under nitrogen was added $Pd(OAc)_2$ (30 mg), PPh_3 (90 mg) and CuI (30 mg). After the solution was stirred for 30 min, trimethylsilylacetylene (0.78 mL, 5.45 mmol) was then added and the suspension was stirred for another 30 min in the ice-bath before being warmed to room temperature. After reacting for 30 min at room temperature, the mixture was heated to 50 °C for 24 h. The solution was then allowed to cool to room temperature and the solvents were removed on a rotary evaporator *in vacuo*. The crude product was purified by column chromatography on silica gel eluting with hexane/CH_2Cl_2 (4 : 1, v/v) to provide **L1-TMS** (520 mg, 0.61 mmol, 57%) as a yellow solid. ^{1}H NMR (400 MHz, $CDCl_3$): δ = 7.64–7.62 (m, 2 H, Ar), 7.47–7.45 (m, 2 H, Ar), 7.31–7.26 (m, 4 H, Ar), 7.26–7.24 (m, 3 H, Ar), 6,96–6.94 (m, 2 H, Ar), 5.35–5.29 (m, 1H, CH), 3.85–3.77 (m, 1H, CH_2), 3.15–3.10 (m, 1H, CH_2), 0.26 (s, 9 H, $Si(CH_3)_3$), 0.21 (s, 9 H, $Si(CH_3)_3$) ppm. FAB-MS: *m/z* = 490.4 $[M]^+$.

2.3.4 Synthesis of L1

A mixture of **L1-TMS** (163 mg, 0.33 mmol) and K_2CO_3 (114 mg, 0.85 mmol) in a mixture of methanol (5 mL) and CH_2Cl_2 (20 mL), under a nitrogen atmosphere, was stirred at room temperature overnight. The mixture was added to CH_2Cl_2 (30 mL) followed by washing with water (20 mL) three times and drying over anhydrous Na_2SO_4. After filtration, the solvents were removed on a rotary evaporator *in vacuo*. The crude product was purified by column chromatography on silica gel eluting with hexane/CH_2Cl_2 (6 : 1, v/v) to provide **L1** (68 mg, 0.20 mmol, 61%) as a yellow solid. ^{1}H NMR (400 MHz, $CDCl_3$): δ = 7.68–7.66 (m, 2 H, Ar), 7.51–7.49 (m, 2 H, Ar), 7.34–7.26 (m, 7 H, Ar), 7.00–6.98 (m, 2 H, Ar), 5.37–5.32 (m, 1H, CH), 3.89–3.82 (m, 1H, CH_2) 3.18–3.12 (m, 2 H, CH_2 + C ≡ CH), 2.97 (s, 1H, C ≡ CH) ppm. ^{13}C NMR (100 MHz, $CDCl_3$): δ = 146.83, 144.18, 141.65, 133.08, 132.68, 132.33, 129.31, 127.88, 125.68, 122.23, 113.02, 111.97 (Ar), 84.43, 83.52, 78.67, 75.48 (C ≡ C), 64.00 (Ph-C), 43.26 (CH_2) ppm. FAB-MS: *m/z* = 346.1 $[M]^+$. IR (KBr) (cm^{-1}): $\nu_{(C\equiv C-H)}$ = 3275; $\nu_{(C\equiv C)}$ = 2103.

2.3.5 Synthesis of P1

To a stirred mixture of **L1** (34.6 mg, 0.10 mmol) and *trans*-$[Pt(PBu_3)_2Cl_2]$ (67.0 mg 0.10 mmol) in freshly distilled triethylamine (20 mL) and CH_2Cl_2 (20 mL) solution was added CuI (5 mg). The solution was stirred at room temperature for 24 h under a nitrogen atmosphere. The solvents were removed on a rotary evaporator *in vacuo*. The residue was redissolved in CH_2Cl_2 and filtered through a short aluminum oxide column using the same eluent to remove ionic impurities and catalyst residue. After removal of the solvent, the crude product was washed with hexane three times followed by methanol three times and then repeated

precipitation from CH_2Cl_2/hexane (or CH_2Cl_2/methanol) and dried *in vacuo* to afford polymer **P1** (68.0 mg, 71%) as an off-white solid. ^{1}H NMR (400 MHz, $CDCl_3$): δ = 7.55 (m, 2 H, Ar), 7.32–7.26 (m, shielded by $CHCl_3$ proton, 7 H, Ar), 7.08 (m, 2 H, Ar), 6.91–6.88 (m, 2 H, Ar), 5.24 (m, 1H, CH), 3.83–3.76 (m, 1H, CH_2), 3.10–3.08 (m, 1H, CH_2), 2.13–2.09 (m, 12 H, PC_4H_9), 1.60–1.56 (m, 12 H, PC_4H_9), 1.45–1.39 (m, 12 H, PC_4H_9), 0.94–0.88 (m, 18 H, PC_4H_9) ppm. ^{31}P NMR (161 MHz, $CDCl_3$): δ = 3.04 ($^1J_{P-Pt}$ = 2331 Hz) ppm. IR (KBr) (cm^{-1}): $\nu_{(C\equiv C)}$ = 2096.

2.3.6 Synthesis of L2-Br

A mixture of **L1-Br** (675 mg, 1.49 mmol) and activated carbon (350 mg) was suspended in acetic acid (10 mL) and heated to 85 °C for 48 h under a nitrogen atmosphere. After the mixture was cooled down, water (50 mL) was added. The resulting solution was extracted with CH_2Cl_2 (30 mL) three times. The organic layer was combined and dried over anhydrous Na_2SO_4. The solvents were removed on a rotary evaporator *in vacuo*. The crude product was purified by column chromatography on silica gel eluting with hexane/CH_2Cl_2 (1:1, v/v) as eluent to provide **L2-Br** (410 mg, 0.90 mmol, 60%) as a white solid. ^{1}H NMR (400 MHz, $CDCl_3$): δ = 7.78 (d, *J* = 11.4 Hz, 2 H, Ar), 7.56 (d, *J* = 8.5 Hz, 2 H, Ar), 7.47 (d, *J* = 8.7 Hz, 2 H, Ar), 7.37–7.35 (m, 3 H, Ar), 7.28–7.26 (m, shielded by $CHCl_3$ proton, 2 H, Ar), 7.24 (d, *J* = 8.7 Hz, 2 H, Ar), 6.79 (s, 1H, Ar) ppm. ^{13}C NMR (100 MHz, $CDCl_3$): δ = 151.14, 144.58, 138.93, 132.03, 131.79, 131.74, 130.02, 128.70, 128.67, 127.30, 126.50, 122.08, 121.09, 105.49 (Ar) ppm. FAB-MS: *m/z* = 455.1 $[M]^+$.

2.3.7 Synthesis of L2-TMS

L2-TMS was prepared in a similar way as **L1-TMS** eluting with hexane/CH_2Cl_2 (1:1, v/v) to obtain the crude product which was a bit difficult to be purified but was used for the next step without further purification.

2.3.8 Synthesis of L2

Following the similar procedure as **L1**, **L2** was obtained by direct desilylation of **L2-TMS** as a white solid in 60% using hexane/CH_2Cl_2 (1 : 1, v/v) as the eluent. ^{1}H NMR (400 MHz, $CDCl_3$): δ = 7.89–7.87 (m, 2 H, Ar), 7.57–7.55 (m, 2 H, Ar), 7.48–7.46 (m, 2 H, Ar), 7.37–7.32 (m, 5 H, Ar), 7.28–7.26 (m, 2 H, Ar), 6.83 (s, 1H, Ar), 3.14 (s, 1H, C≡CH), 3.12 (s, 1H, C≡CH) ppm. ^{13}C NMR (100 MHz, $CDCl_3$): δ = 151.45, 144.63, 140.01, 133.18, 132.74, 132.50, 130.15, 128.74, 128.66, 125.59, 124.76, 121.61, 121.08, 105.89 (Ar), 83.68, 82.81, 78.24, 77.85 (C≡C) ppm. FAB-MS: *m/z* = 344.2 $[M]^+$. IR (KBr) (cm^{-1}): $\nu_{(C\equiv C-H)}$ = 3272; $\nu_{(C\equiv C)}$ = 2107.

2.3.9 Synthesis of P2

Like **P1**, **P2** was obtained as an off-white solid in 67% from **L1**. ^{1}H NMR (400 MHz, $CDCl_3$): δ = 7.78–7.76 (m, 2 H, Ar), 7.31–7.19 (m, shielded by the $CHCl_3$ proton, 11 H, Ar) 6.78 (s, 1H, Ar), 2.14 (m, 12 H, PC_4H_9), 1.8 (m, 12 H, PC_4H_9), 1.46–1.44 (m, 12 H, PC_4H_9), 0.94–0.91 (m, 18 H, PC_4H_9) ppm. ^{31}P NMR (161 MHz, $CDCl_3$): δ = 3.01 ($^1J_{P-Pt}$ = 2334 Hz) ppm. IR (KBr) (cm^{-1}): $\nu_{(C\equiv C)}$ = 2098.

3 Results and Discussion

3.1 Synthesis and Characterization of Pt(II) Complexes

The chemical structure and synthetic routes of the polymers **P1** and **P2** are shown in Schemes 1 and 2, respectively. The key compound, **L1-Br**, was prepared by the ring closure reaction between (4-bromophenyl)hydrazine chloride and 1-(4-bromophenyl)-3-phenylprop-2-en-1-one in ethanol as a yellow solid. Ethanol was chosen as the solvent at the refluxing temperature to ensure the dissolution of the reactants and precipitation of the cyclized products. The use of acetic acid catalysts favours cyclization as opposed to the formation of phenylhydrazone derivatives of Michael addition products [27]. Following the general mechanism proposed by Coispeau and Elguero [28], 1,2-addition of the primary nitrogen atom of the phenylhydrazine occurs at the carbonyl group of ketone compound, followed by cyclization by means of an electrocyclic reaction involving six electrons. Conversion of the dibromide compound to its corresponding diethynyl congener (**L1**) via **L1-TMS** can be readily achieved following the typical organic synthetic protocols for alkynylation of aromatic halides followed by deprotection reaction using a base [29]. Polymer **P1** was prepared by the Sonogashira-type dehydrohalogenation reaction between the diethynyl precursor (**L1**) and *trans*-$[Pt(PBu_3)_2Cl_2]$ with the feed mole ratio of 1:1 [3–5, 30]. It was carefully purified to remove ionic impurities and catalyst residues, and repeated precipitation and isolation led to an off-white solid with good yield and high purity.

Scheme 2 shows the chemical structure and synthetic strategy of **P2**. Polymer **P2** was prepared from the dibromo precursor **L2-Br** using the same method as **P1**. Firstly, **L2-Br** was prepared from **L1-Br** as a white solid *via* the carbon-catalyzed oxidation reaction [31], which can then be ethynylated to give **L2**. Polymer **P2** was similarly prepared

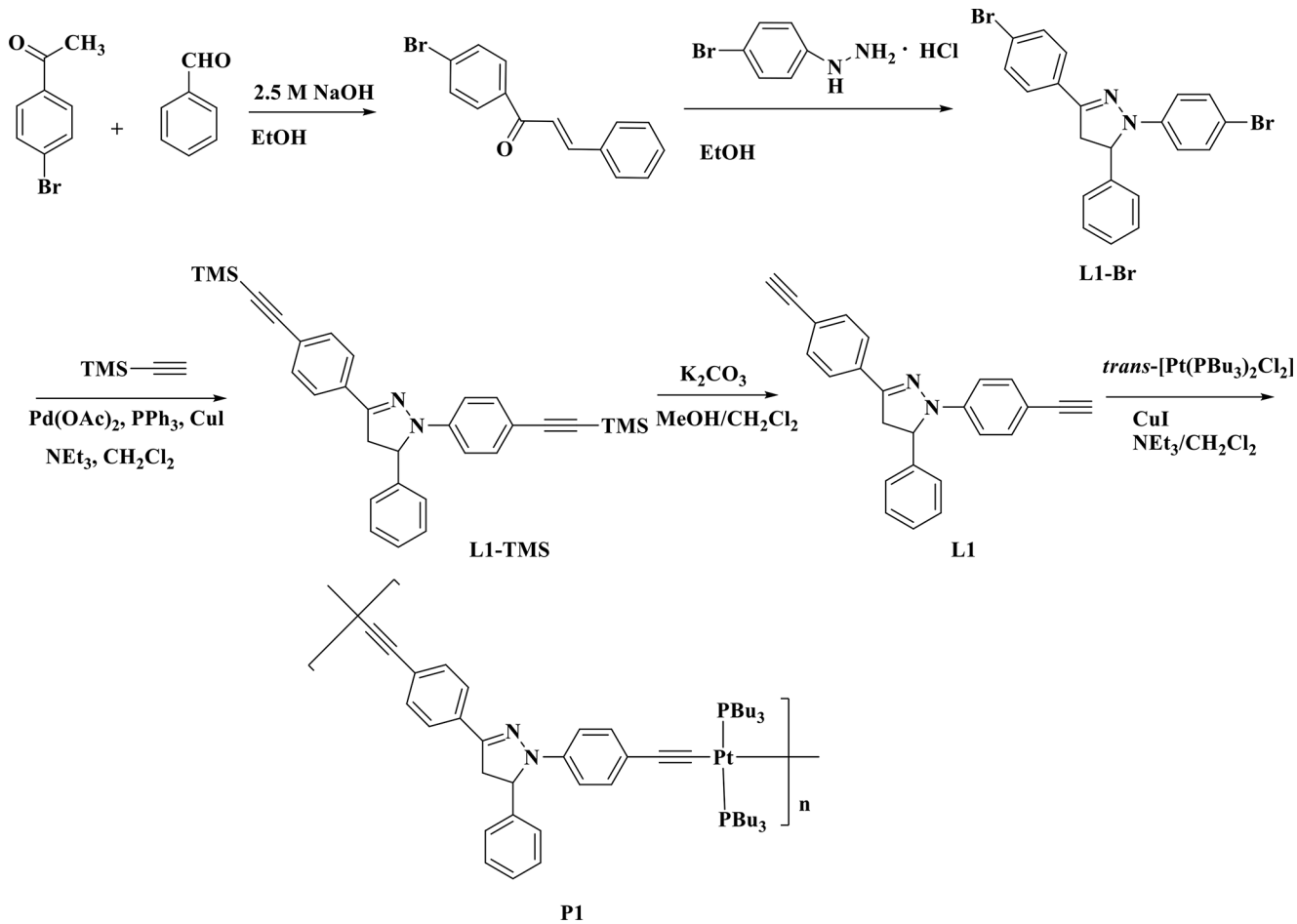

Scheme 1 The synthetic pathway of **P1**

as an off-white solid *via* the Sonogashira-type dehydrohalogenation reaction between the diethynyl precursor (**L2**) and *trans*-[Pt(PBu$_3$)$_2$Cl$_2$].

The chemical structures of the Pt(II) complexes and polymers were verified by NMR (^{1}H and ^{31}P) and IR spectroscopy. The single ^{31}P-{^{1}H} NMR signal flanked by platinum satellites for each of the metallopolymers is consistent with a *trans* arrangement of the Pt(PBu$_3$)$_2$ unit in the square-planar geometry. The $^1J_{P-Pt}$ values of 2331–2334 Hz for the PBu$_3$ moieties are typical of those for related *trans*-PtP$_2$ systems [32, 33]. All the terminal alkynyl ligands and Pt(II) compounds display vibrational frequencies of the acetylenic functional groups clearly. In the IR spectra of the diethynyl ligands **L1** and **L2**, they show IR $\nu_{C\equiv C}$ absorption at around 2103–2107 cm^{-1}. The corresponding terminal acetylenic C≡C–H stretching vibrations occur at around 3272–3275 cm^{-1}. The C≡C stretching frequencies for **P1**–**P2** are lower than those for **L1**-**L2**, in line with a higher degree of conjugation in the polymers [34].

Using gel-permeation chromatography (GPC), the number-average molecular weights (M_n) of **P1** and **P2** were estimated to be 28,890 and 30,075, respectively, calibrated against polystyrene standards (Table 1). Their polydispersity indexes (PDI) in the narrow range of 1.24–1.49 are consistent with the proposed linear structure from the condensation polymerization [3]. It is known that GPC does not give absolute molecular weights but provides a measure of hydrodynamic volume. We expect a notable difference in the hydrodynamic behavior between rigid-rod type polymers in solution and flexible polymers. So, these molecular weights may be overestimated, leading to certain systematic errors in the GPC data.

3.2 Thermal, Optical and Redox Properties

Both polymers are thermally and air-stable solids and they are soluble in common organic solvents. From the curves in thermal gravimetric analysis (TGA), the respective percent weight loss indicates the removal of one PBu$_3$ and some of the Bu groups from their polymers in the decomposition step. Decomposition onset was defined by a 5 wt.-% loss in each case. The onset decomposition temperatures of 322 °C (**P1**) and 348 °C (**P2**) are notably higher than those

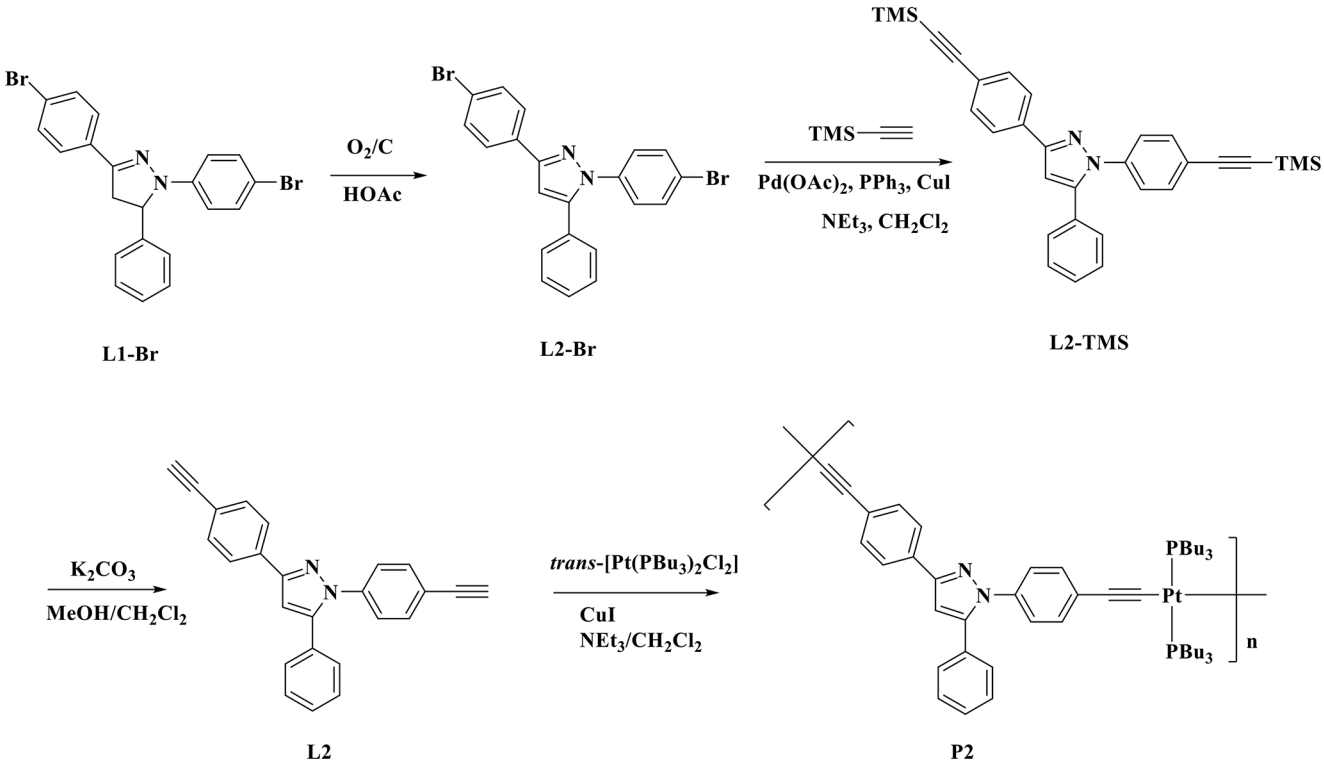

Scheme 2 The synthetic pathway of **P2**

Table 1 GPC and TGA data of **P1**–**P2**.

Polymer	M_n [a]	M_w [b]	PDI[c]	DP[d]	T_{dec} [°C]
P1	28,890	35,870	1.24	31	322
P2	30,075	44,830	1.49	32	348

[a] M_n = Number-average molecular weight

[b] M_w = Weight-average molecular weight

[c] PDI = Polydispersity index

[d] DP = Degree of polymerization (calculated from M_n values)

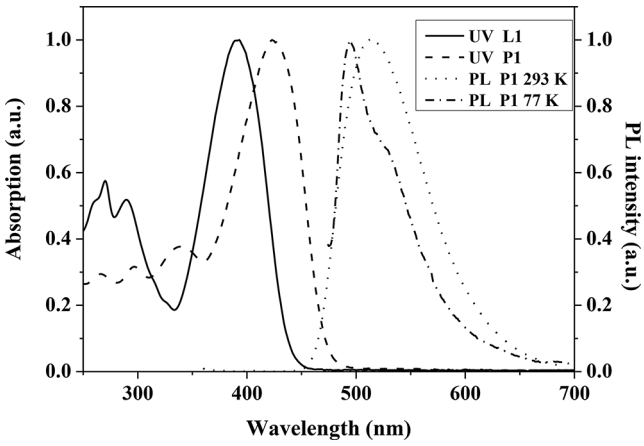

Fig. 1 Normalized absorption and emission spectra of **L1** and **P1** in CH_2Cl_2 solution at 293 K and 77 K

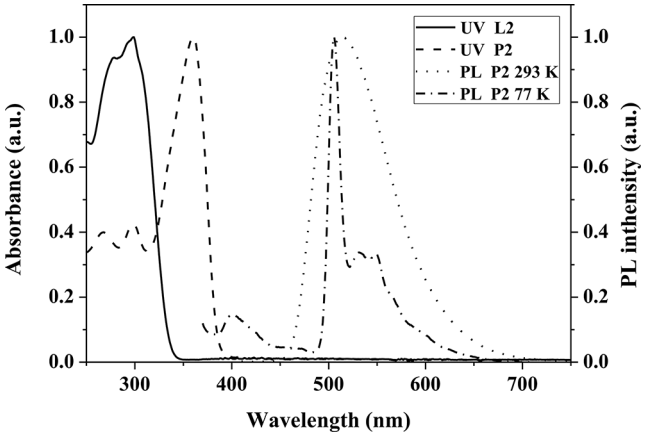

Fig. 2 Normalized absorption and emission spectra of **L2** and **P2** in CH_2Cl_2 solution at 293 K and 77 K

for the polymers with diphenyl (297 °C) [35] and dipyridyl (274 °C) [36] moieties.

The polymers **P1** and **P2** exhibit different absorption properties. Figure 1 shows the UV/Vis absorption of **L1** and **P1** and PL emission spectra of **P1** at 293 K and 77 K. Those of **L2** and **P2** are depicted in Fig. 2. The absorption spectrum of **L1** is characterized by a broad and featureless band peaking at 391 nm which can be assigned to a ligand-centered π-π* transition. The other one below 300 nm is the characteristic absorption peak of the triaryl-pyrazoline group. However, **L2** only shows one peak below 300 nm,

Table 2 Photophysical data of **P1**–**P2**.

	Absorption (293 K)	Emission (293 K)				Emission (77 K)	
	λ_{abs} [nm] CH_2Cl_2[a]	Bandgap E_g [eV][b]	λ_{em} [nm] CH_2Cl_2	Φ (%)[c]	τ_P (ns)	λ_{em} [nm] CH_2Cl_2	τ_P (μs)
P1	265*, 297*, 339*, 423	2.60	514	0.032	0.66	494, 528*	69.9
P2	268*, 298*, 360	3.20	515	0.028	0.58	401*, 506, 531*, 548*	78.9

[a] Asterisk refers weak or shoulder peak

[b] Optical bandgaps determined from the onset of absorption in solution phases

[c] Against a 0.5 M H_2SO_4 solution of quinine sulfate as a reference

Table 3 Redox potentials and frontier orbital energy levels of the polymers **P1** and **P2**

Polymer	Oxidation potential (V)	Energy levels (eV)		Bandgap (eV)
	$E_{onset,\ ox}$[a]	E_{HOMO}[b]	E_{LUMO}[c]	E_g^{opt}[d]
P1	+0.64	-5.36	-2.76	2.60
P2	+1.12	-5.84	-2.64	3.20

[a] $E_{onset,\ ox}$ are the onset potentials of oxidation

[b] $E_{HOMO} = -(E_{onset,\ ox} + 4.72)$ eV

[c] Calculated from the optical bandgap and the energy level of HOMO and $E_{LUMO} = (E_{HOMO} + E_g^{opt})$ eV

[d] E_g^{opt} = Optical bandgap as estimated from the absorption onset in the solution state ($E_g^{opt} = 1240/\lambda_{abs}^{onset}$ eV)

which is due to the pyrazolyl group. The absorption bands of **P1** and **P2** have a significant red shift compared to those of the corresponding ligands, which can be attributed to the extension of metal-organic π-conjugation length in the presence of heavy platinum unit.

P1 and **P2** show similar broad and structureless emission peaks at around 514 nm arising from the singlet excited state at 293 K. The PL quantum yields of **P1** and **P2** in CH_2Cl_2 were measured to be 3.2 and 2.8%. The measured PL lifetimes for **P1** and **P2** for the main peaks are all very short (ca. 0.58–0.66 ns) at 293 K, characteristic of the spin-allowed singlet emission [1, 3]. With reference to other pyrazole derivatives in the literature, since this emission peak is observed with a significant Stokes shift, the absorption transition probably consists of π-π* origin with some charge transfer character to establish a lower-energy twisted intramolecular charge-transfer state [37]. A strong π-π* triplet emission at around 494 and 506 nm, with a triplet emissive lifetime τ_P of ca. 69.9 μs and 78.9 μs, is detectable from the PL spectrum of **P1** and **P2** at 77 K, respectively. The long lifetime is caused by the heavy metal center which induces strong spin-orbit coupling, and then increases the phosphorescence [1, 3]. The small peak at 401 nm for **P1** is due to the weak π-π* fluorescence emission, typical of other Pt-polyynes reported in the literature [38, 39].

Both polymers undergo a rigidochromic blue shift in the emission wavelength upon cooling of their solutions to 77 K. The hypsochromic shift observed at low temperature is mainly caused by the solvent reorganization in a fluid solution at 77 K that can readily stabilize the charge transfer states prior to emission [40]. This process is significantly impeded in a rigid matrix at 77 K, and hence fluorescence appears at a higher energy. The absence of vibronic progression in the emission profile (at 293 K) suggests mostly a charge-transfer state but not the ligand-centered π-π* excited state. The observed emission lifetimes (τ) of our platinum compounds at 77 K are longer than those measured at room temperature [41] (Table 2).

The HOMO and LUMO levels of the polymers **P1**–**P2** were calculated based on the redox potentials determined from electrochemical measurements using cyclic voltammetry. The key data are gathered in Table 3. From the onset values of oxidation potential ($E_{onset,\ ox}$), the HOMO levels of the polymers were calculated according to the equation $E_{HOMO} = -(E_{onset,\ ox} + 4.72)$ eV where the unit of potential is V versus Ag/AgCl while the LUMO levels were determined from the optical bandgap and the energy level of HOMO using the equation $E_{LUMO} = (E_{HOMO} + E_g^{opt})$ eV [42, 43]. **P1** shows an irreversible oxidation wave at 0.64 eV while **P2** shows an oxidation wave at 1.12 eV. **P1** shows an elevated HOMO level (-5.36 eV) relative to **P2** (-5.84 eV), indicating that **P1** is more electropositive (or has a lower ionization potential) than **P2**, and hence a better hole transport ability in **P1** would be anticipated.

3.3 Photovoltaic Properties

Since the light-induced intramolecular electron transfer could easily occur from donor to acceptor through the π-conjugation which favours photocurrent generation and the photoelectronic energy conversion in photovoltaic devices, PSCs with BHJ configuration were fabricated by using **P1** with better absorption properties as electron donor and PCBM as electron acceptor. The hole collection electrode consisted of indium tin oxide (ITO) with a spin-coated poly(3,4-ethylene-dioxythiophene):poly(styrene sulfonate) (PEDOT:PSS), while Al served as the electron collecting electrode. Figure 3 shows the *J-V* curve of PSCs with **P1**:PCBM (1:4, w/w) active layers under simulated AM1.5 solar irradiation. A PCE of 0.27% can be obtained for **P1** with V_{oc} = 0.63 V, J_{sc} = 1.33 mA cm^{-2} and FF = 0.32 under illumination of an AM 1.5 solar cell simulator.

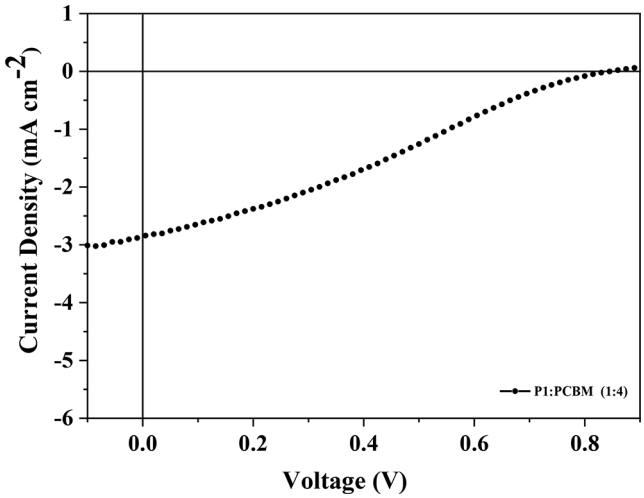

Fig. 3 *J-V* curve of PSC with **P1**:PCBM (1:4 w/w) active layer under simulated AM 1.5 solar irradiation

4 Conclusion

In summary, two new platinum-containing polymetallayne polymers functionalized with pyrazoline and electron-rich pyrazole moieties have been successfully synthesized *via* Sonogashira-type dehydrohalogenation polycondensation reaction. All of them exhibit good solubility in common organic solvents and good thermal stability and show different absorption properties in the visible region. This observation showcases that the energy level and bandgap of the polymers could be effectively tuned by changing the number of double bonds of the five-membered ring of the pyrazoline derivative. It is found that the use of pyrazole down-shifted the HOMO energy level by ca. 0.48 eV and blue-shifted the absorption profile of the conjugated polymer as compared to the corresponding pyrazoline counterpart. These results reveal that molecular control by using pyrazoline instead of pyrazole ring would broaden the absorption and up-shifting the HOMO level, hence improving the photovoltaic property of PSCs.

Acknowledgements W.-Y. W. thanks the financial support from the RGC Senior Research Fellowship Scheme (SRFS2021-5S01), the National Natural Science Foundation of China (52073242), the Hong Kong Research Grants Council (PolyU 15307321), Research Institute for Smart Energy (CDAQ) and Miss Clarea Au for the Endowed Professorship in Energy (847 S). Q. W. and J. L. thank the financial support from Chengdu University. Z. S. thanks the financial support from the Hong Kong Polytechnic University (1-BDTU).

Author Contributions Qiwei Wang: conceptualization, investigation, resources, supervision, writing-original draft; Lu Jiang: data curation, investigation; Junlong Li: data curation, funding acquisition; Zelin Sun: funding acquisition, writing-review & editing; Wai-Yeung Wong: funding acquisition, project administration, resources, supervision, writing-review & editing.

Funding Open access funding provided by The Hong Kong Polytechnic University

Data Availability No datasets were generated or analysed during the current study.

Declarations

Competing Interests The authors declare no competing interests.

Open Access This article is licensed under a Creative Commons Attribution 4.0 International License, which permits use, sharing, adaptation, distribution and reproduction in any medium or format, as long as you give appropriate credit to the original author(s) and the source, provide a link to the Creative Commons licence, and indicate if changes were made. The images or other third party material in this article are included in the article's Creative Commons licence, unless indicated otherwise in a credit line to the material. If material is not included in the article's Creative Commons licence and your intended use is not permitted by statutory regulation or exceeds the permitted use, you will need to obtain permission directly from the copyright holder. To view a copy of this licence, visit http://creativecommons.org/licenses/by/4.0/.

References

1. A. Haque, R.A. Al-Balushi, I.J. Al-Busaidi, M.S. Khan, P.R. Raithby, Chem. Rev. **118**, 8474–8597 (2018)
2. P.D. Harvey, J. Inorg. Organomet. Polym. Mater. **27**, S3–S38 (2017)
3. C.-L. Ho, Z.-Q. Yu, W.-Y. Wong, Chem. Soc. Rev. **45**, 5264–5295 (2016)
4. C.-L. Ho, W.-Y. Wong, Coord. Chem. Rev. **257**, 1614–1649 (2013)
5. W.-Y. Wong, C.-L. Ho, Coord. Chem. Rev. **250**, 2627–2690 (2006)
6. A. Haque, L. Xu, R.A. Al-Balushi, M.K. Al-Suti, R. Ilmi, Z. Guo, M.S. Khan, W.-Y. Wong, P.R. Raithby, Chem. Soc. Rev. **48**, 5547–5563 (2019)
7. W.-Y. Wong, Dalton Trans. 4495–4510 (2007)
8. W.-Y. Wong, P.D. Harvey, Macromol. Rapid Commun. **31**, 671–713 (2010)
9. W.-Y. Wong, C.-L. Ho, Acc. Chem. Res. **43**, 1246–1256 (2010)
10. A. Haque, R.A. Al-Balushi, M.S. Khan, J. Organomet. Chem. **897**, 95–106 (2019)
11. G.-J. Zhou, W.-Y. Wong, Chem. Soc. Rev. **40**, 2541–2566 (2011)
12. W.-Y. Wong, J. Inorg. Organomet. Polym. Mater. **15**, 197–219 (2005)
13. J. Barberá, K. Clays, R. Giménez, S. Houbrechts, A. Persoons, J.L. Serrano, J. Mater. Chem. **8**, 1725–1730 (1998)
14. M. Mehkoom, S.M. Afzal, S. Ahmad, S.A. Khan, J. Mol. Liq. **345**, 117018 (2022)
15. M. Khalid, A. Mustafa, S. Ahmed, M.A. Asghar, T. Ahamad, A.A. Braga, S.C. Ojha, Arab. J. Chem. **16**, 105271 (2023)
16. M. Parshad, D. Kumar, V. Verma, Inorg. Chim. Acta. **560**, 121789 (2024)
17. J.O. Morley, D. Pugh, in Organic Materials for Nonlinear Optics, ed. R. A. Hann and D. Bloor, Spec. Publ. R. Soc. Chem. 69, Kent, 1989, p. 28
18. E. David, K. Mishra, K. Thirumoorthy, N. Palanisami, Appl. Organomet. Chem. **35**, e6138 (2021)

19. Y.S. Xie, X.-H. Pan, B.-X. Zhao, J.-T. Liu, D.-S. Shin, J.-H. Zhang, L.-W. Zheng, J. Zhao, J.-Y. Miao, J. Organomet. Chem. **693**, 1367–1374 (2008)
20. K. Senthilkumar, K. Thirumoorthy, G. Vinitha, K. Soni, N.S.P. Bhuvanesh, N. Palanisami, J. Mol. Struct. **1128**, 36–43 (2017)
21. M. Pokladko-Kowar, E. Gondek, A. Danel, T. Uchacz, P. Szlachcic, K. Wojtasik, P. Karasinski, Crystals. **12**, 434 (2022)
22. C.-Q. Ma, L.-Q. Zhang, X.-H. Li, X.-S. Wang, B.-W. Zhang, Y. Cao, D.-M. Wang, X.-Y. Jiang, Z.-L. Zhang, D.-Q. Zhang, Y. Qiu, Acta Chim. Sinica. **60**, 847–853 (2002)
23. C.-Q. Ma, L.-Q. Zhang, J.-H. Zhou, X.-S. Wang, B.-W. Zhang, Y. Cao, P. Bugnon, M. Schaer, F. Nüesch, D.-Q. Zhanga, Y. Qiu, Chin. J. Chem. **20**, 929–932 (2002)
24. D. Xiao, L. Xi, W. Yang, H. Fu, Z. Shuai, Y. Fang, J. Yao, J. Am. Chem. Soc. **125**, 6740–6475 (2003)
25. V. Mukundam, S. Sa, A. Kumari, T.T. Ponduru, R. Das, K. Venkatasubbaiah, Chem. Asian J. **17**, e202200291 (2022)
26. G.B. Kauffman, L.A. Teter, Inorg. Synth. **7**, 245–249 (1963)
27. R.S. Theobald, in Rodd's Chemistry of Carbon Compounds, 2nd Edition, ed. S. Coffey and M. F. Ansell, Vol. 4, Heterocyclic Compounds, Part C, ed. M. F. Ansell, Elsevier, New York, 1986, ch. 1
28. G. Coispeau, J. Elguero, Bull. Soc. Chim. Fr. 2717–2736 (1970)
29. S. Takahashi, Y. Kuroyama, K. Sonogashira, N. Hagihara, Synthesis 627–630 (1980)
30. W.-Y. Wong, C.K. Wong, G.L. Lu, A.W.M. Lee, K.W. Cheah, J.X. Shi, Macromolecules. **36**, 983–990 (2003)
31. N. Nakamichi, Y. Kawashita, M. Hayashi, Synthesis. **7**, 1015–1020 (2004)
32. W.-Y. Wong, C.K. Wong, G.L. Lu, K.W. Cheah, J.X. Shi, Z. Lin, J. Chem. Soc. Dalton Trans. 4587–4594 (2002)
33. Q. Wang, W.-Y. Wong, Polym. Chem. **2**, 432–440 (2011)
34. J. Lewis, N.J. Long, P.R. Raithby, G.P. Shields, W.-Y. Wong, M. Younus, J. Chem. Soc. Dalton Trans. 4283–4288 (1997)
35. L. Liu, S.-Y. Poon, W.-Y. Wong, J. Organomet. Chem. **690**, 5036–5048 (2005)
36. M.S. Khan, M.R.A. Al-Mandhary, M.K. Al-Suti, A.K. Hisahm, P.R. Raithby, B. Ahrens, M.F. Mahon, L. Male, E.A. Marseglia, E. Tedesco, R.H. Friend, A. Köhler, N. Feeder, S.J. Teat, J. Chem. Soc. Dalton Trans. 1358–1368 (2002)
37. S.K. Liew, A. Holownia, A.J. Tilley, E.I. Carrera, D.S. Seferos, A.K. Yudin, J. Org. Chem. **81**, 10444–10453 (2016)
38. W.-Y. Wong, G.-L. Lu, K.-H. Choi, J.-X. Shi, Macromolecules. **25**, 3506–3513 (2002)
39. N. Chawdhury, A. Köhler, R.H. Friend, W.-Y. Wong, J. Lewis, M. Younus, P.R. Raithby, T.C. Corcoran, M.R.A. Al-Mandhary, M.S. Khan, J. Chem. Phys. **110**, 4963–4970 (1999)
40. A.B. Tamayo, S. Garon, T. Sajoto, P.I. Djurovich, I.M. Tsyba, R. Bau, M.E. Thompson, Inorg. Chem. **44**, 8723–8732 (2005)
41. C.-L. Ho, W.-Y. Wong, G.-J. Zhou, B. Yao, Z. Xie, L. Wang, Adv. Funct. Mater. **17**, 2925–2936 (2007)
42. J. Hou, Z. Tan, Y. Yan, Y. He, C. Yang, Y. Li, J. Am. Chem. Soc. **128**, 4911–4916 (2006)
43. C.G. Van de Walle, J. Neugebauer, Nature. **423**, 626–628 (2003)

Publisher's Note Springer Nature remains neutral with regard to jurisdictional claims in published maps and institutional affiliations.